SWELL PROPAGATION AND NEARSHORE WAVE CLIMATE

Douglas Scott[1], Donald Resio[2] and Cristobal Pantoja[3]

1. Baird & Associates, Ottawa, Ontario
2. U.S. Army ERDC, Vicksburg, MS
3. Baird & Associates, Santiago, Chile

1. INTRODUCTION

A detailed study of swell wave conditions in the southern Pacific Ocean has been performed with particular emphasis on the western Southern American coastline. This study was one part of an overall wave hindcasting investigation undertaken for the Servicio Hidrografico y Oceanográfico de la Armada de Chile (SHOA) to define the inshore wave climate at various locations along the Chilean seabord.

Considerable coastal infrastructure has been developed in Chile over the last two decades, and the impetus for this study was based on concerns with the lack of consistency utilized in the coastal engineering design process, beginning with, but not limited to, the definition of the wave conditions. The available wave records in Chile are of very limited duration, thus many designers rely on a variety of wave data sources ranging from ship observations to hindcast wave data of various types and flavours. One of the major issues identified was that engineering structures have often been developed using data with relatively simplistic wave definitions, employing integrated wave parameters, such as the characteristic wave height (Hm0), peak wave period (Tp) and the mean wave direction (MWD). As will be shown in this paper, the wave climate in Chile is complex and it is important that appropriately complex wave analysis techniques be employed.

It has also been long recognized in Chile that swell waves are a critical consideration in assessing the performance of ports, and several of the ports in Chile do experience downtime due to excessive vessel motion induced by long-period swells and harbour resonance phenomenon. An important consideration is the ability to estimate the magnitude and frequency of swell waves.

In support of this study, a forty-year wave hindcast was completed for the Pacific Ocean using a 2nd Generation wave model and the NCEP/NCAR Re-Analysis wind fields. Some of the key wave modelling challenges addressed included:

- Undertaking a long-term wave hindcast in data-poor environment.
- The appropriate reproduction of the wind fields in intense extratropical cyclones of the Northern and Southern Pacific Ocean.
- The simulation of swell propagation using wave models having limited directional resolution.

This paper summarizes the methodology and findings of the study.

2. REGIONAL SETTING

Chile is a long, relatively thin country that stretches along the western edge of the Southern American continent, as may be seen in Figure 1. It experiences large meteorological variability along this length. The climate varies from arid desert in the north at latitude 17 ° S to a much colder and wetter environment in the south at latitude 56° S. An important topographic feature is the presence of the Andes mountain chain that runs down the eastern edge of the country. In the northern half of the country, atmospheric circulation is largely controlled by the South Pacific High, resulting in winds blow parallel to the coast north of approximately 31° S. Further south, the winds take a more westerly direction. In the zone of sub-Antarctic depressions (south of ~42°), average wind speeds increase considerably and there is a more complete western dominance to the wind direction.

Similar to the meteorological setting, the incident wave climate shows considerable variability, with the following principal considerations:

- Seas generated by the local wind conditions, which vary along the length of the country.
- Swells generated in the southern mid-latitudes by the passage of cyclonic systems. These swells, in combination with the locally generated seas, are an important consideration in establishing the design conditions for coastal structures.
- Swells generated in the northern mid-latitudes, which propagate some 15,000 km to impact the Chilean coastline.
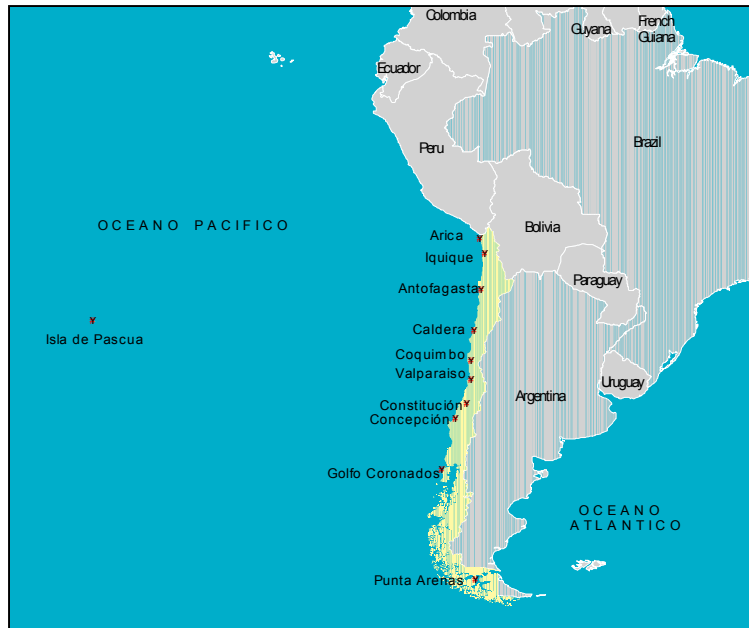

Figure 1. Location Plan

As will be shown in this paper, the long period wave energy in Chile, particularly in the northern part of the country, is a seasonal interplay between the swells propagating from the northern and southern hemispheres.

Many of the existing ports in Chile are located in north-facing bays and are well protected from the southern seas and swells, but can be highly exposed to northern swells. Figure 2 shows one typical example, at the Port of Mejillones in Bahia de Mejillones, which is located at approximately 24° S. The importance of northern swells may be seen in a short duration of wave records made in 10 m depth within the bay, as illustrated in Figure 3. This site is almost completely sheltered from southern to western wave conditions, and the northern swells can be readily isolated. The wave record shows the distinctive "sawtooth" pattern of swell generated by distant storm events. Plotting the time series as a function of frequency and calculating the slope of the wave period progression, permits an estimate of the time and distance to the generating storm to be developed. In this case, the storms were estimated to be located in the order of 12,000 km to 15,000 km from the site.
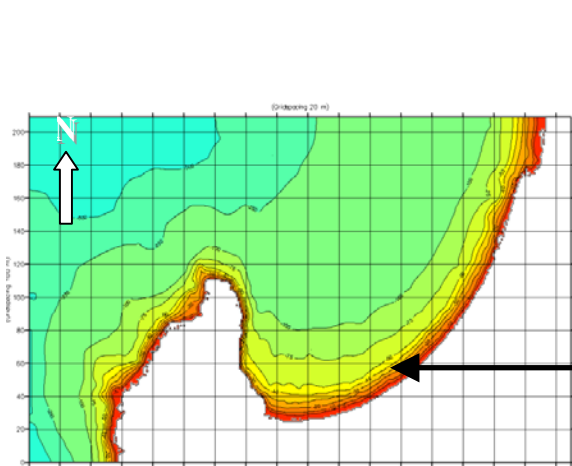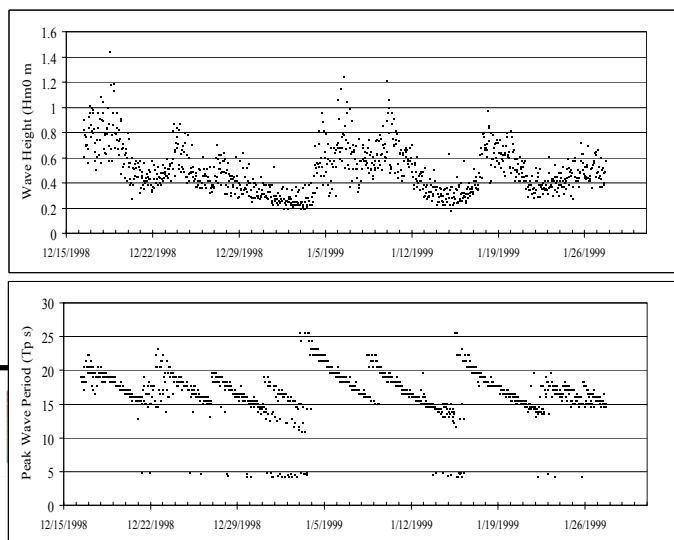

Figure 2. Mejillones Bay

Figure 3. Wave Records in Mejillones Bay

3.	AVAILABLE WAVE DATA

3.1 Regional Wave Buoy Measurements

Historical wave data for the eastern Pacific Ocean in the Southern Hemisphere are limited. The SHOA have measured waves at a variety of locations along the Chilean coastline over the past 20 years, as shown in Table 1 (organized from north to south) and Figure 4. Most of these wave records have duration of one year or less, and generally the wave buoy was placed in shallow water.   Most of the historical observations were performed using Datawell non-directional Waveriders; however, more recently (2000 onwards) the wave measurements have been conducted by means of a TriAxys directional buoy.

In addition to the SHOA buoys, the U.S. National Oceanic and Atmospheric Administration (NOAA) operated a non-directional 3 metre discus buoy to the west of northern Chile at location 18.0° S and 85.1° W. Wave measurements were conducted at this buoy from 1986 to 1995.

Wave data from NOAA buoys in the North Pacific, such as NOAA 46003 near the Aleutian Islands, and NOAA buoys 46059 and 46042 near California, were also employed in the study for hindcast model validation.

Table 1
Historical Wave Measurements Conducted in Chile

Location	Start	End	Water Depth	Median Hm0 (m)	Median Tp (s)
Arica	07/07/88	07/07/89	051 m	1.42	15.5
Iquique	05/06/87	12/07/88	072 m	1.40	15.6
Antofagasta	15/10/90	05/12/91	100 m	1.34	12.2
Caldera	22/08/82	27/01/84	095 m	0.92	15.7
	12/12/87	20/04/88	097 m		
Isla de Pascua	23/06/82	20/12/82	097 m	1.75	13.2
	05/01/83	23/01/83	097 m		
	18/04/92	05/08/92	097 m		
	21/09/92	07/10/92	097 m		
	04/11/92	12/03/93	097 m		
	12/03/93	16/09/93	097 m		
Coquimbo	17/08/89	10/10/90	108 m	1.49	14.3
Valparaíso	06/07/79	10/12/79	105 m	1.70	14.7
	02/05/81	08/13/81	105 m		
	01/06/00	29/09/00	110 m	2.00	12.1
	06/04/01	27/08/01	135 m		
Constitucion	18/02/84	22/02/85	107 m	1.78	14.2
San Vicente	29/10/85	05/02/86	022 m	0.96	16.3
Golfo Coronados	13/05/86	11/06/87	051 m	2.30	13.2
Faro Félix	02/05/92	26/04/93	098 m	1.86	10.9

There is generally an increasing trend in median wave height from north to south for those buoys that had a reasonable degree of open exposure (Arica, Iquique, Valparaiso, Constitucion, Golfo Coronados).
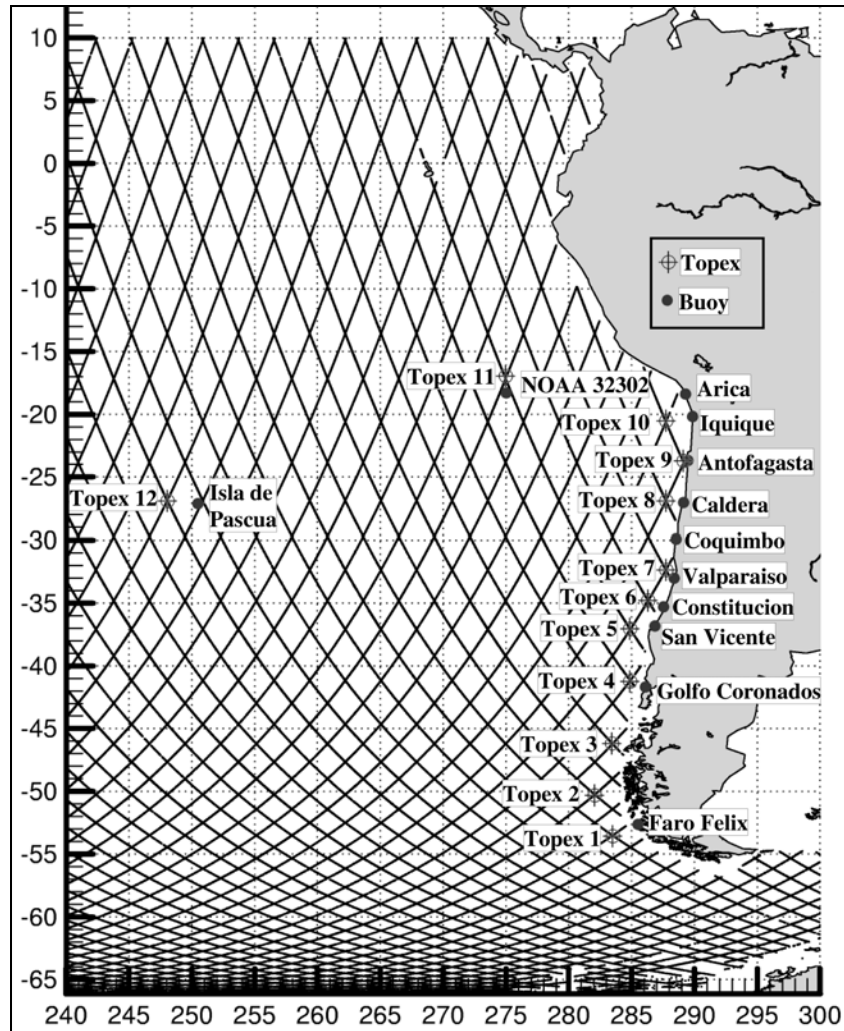
Figure 4. Locations of Regional Wave Measurements
[Lines Show Topex Ascending/Descending Tracks]

3.2 Satellite Altimeter Measurements

Satellite altimeter wave data from the Topex/Poseidon mission were used extensively in the wave climate study. Several quality control procedures were applied to the altimeter data in order to eliminate spurious measurements prior to statistical analysis of the data. The data were also corrected for Side A drift from April 1, 1997 to January 31, 1999, and for the new calibration that resulted when the Side B sensor became active (Cotton, 2001). The satellite data were derived from the average wave height measurement in each satellite pass through a 0.5-degree box centered at satellite crossover locations. Data from a total of 12 different locations were considered, as shown in Figure 4.

4.   APPLICATION OF THE WAVE MODEL

4.1 Model Description

The WAVAD wave model, as summarized in Resio (1981) and Resio and Perrie (1989), was used for all of the hindcasting carried out in this study. WAVAD is a second generation (2G) spectral wave model that maintains an equilibrium between the wind source and non-linear wave energy flux with an assumed f^4 shape for the wave spectrum. The non-linear wave interactions are represented as a momentum flux to the forward face (frequencies

less than spectral peak) of the spectrum based on a constant proportion of the energy transferred out of the mid-range frequencies. Wave-wave interactions also transfer energy to the high frequency region of the spectrum where it is assumed that energy is lost due to breaking processes. Wave propagation was handled in the original WAVAD model by means of a first order upwinding scheme, although this was subsequently altered as discussed in Section 5.

The numerical model grid covered a domain extending from 120° E to 66° W and from 64° S to 56° N with a resolution of 1.0°. The model bathymetry for much of the Pacific Ocean was derived from a global (ETOPO30) database.   A total of twenty-three frequencies were used for the hindcasts in conjunction with a directional resolution of 22.5° (16 direction bands). The frequencies were spaced at a constant ratio of 1.1 starting at 0.038 Hz.

Ice coverage was included in the model using NCEP/NCAR ice data, and was updated on a 6-hourly basis throughout the duration of the hindcast.

A forty-year hindcast (1961-2000) was performed. The hindcast model output was archived every two hours at grid points along the Chilean coastline and at each of the data comparison points. Both the full directional spectra as well as files containing the integrated summary parameters were stored at each of the archival points. Special compression algorithms were developed to efficiently handle the directional spectra by only storing those direction-frequency bins containing energy above a pre-determined minimum threshold.

4.2 The Wind Field

Wind fields derived from the NCEP/NCAR Reanalysis Project data set (Kalanay et al., 1996) were used as the primary driving mechanism for the wave model.   The U (east-west) and V (north-south) wind fields at 10 m elevation above ground were extracted from the NCEP/NCAR global database for a grid network that covered the entire Pacific Ocean. The NCEP data are available on a 6-hourly basis for a grid resolution of 1.875° longitude by an average 1.905° latitude (actual grid is Gaussian), and were interpolated onto the more refined WAVAD input grid using a four-point bi-linear interpolation scheme. This approach provided a driving wind field for the model at six-hour intervals. The WAVAD model automatically interpolated the six-hour wind fields to the selected model time step of two hours.

5.   KEY MODELLING ISSUES

5.1 Systematic Correction of Extratropical Cyclone Winds

It has been recognized (e.g. Cox, 2000) that the NCEP/NCAR winds under-estimate wind speeds in larger storm events as the limited resolution of the meteorological model cannot fully represent the complexities of a storm event. In this case, as the focus was on swell events generated by mid-latitude extratropical cyclones, it was important to develop some means for a systematic correction the winds generated by these cyclones. Traditional approaches to improving the wind field representation, such as kinematic analysis, are not truly feasible due to the limited meteorological observation network in the southern Pacific Ocean. For this study, various assessments were performed, including:

- Comparison of the NCEP/NCAR storm wind structure to that provides by scatterometer data, such as Quikscat. Although initial promising, the data handling and manipulation required for this level of effort quickly proved beyond the scope of the project.
- Use of wind speed estimates derived from satellite altimeters did not provide useful due to the potentially low saturation limits of these sensors with respect to wind speed estimation.

Ultimately, a relatively simple approach was developed based on comparisons of the hindcast model results to Topex data. Altimeter estimates of wave heights over the period 1992 to 2000 were derived from two distinct storm generating regions of the Pacific Ocean: (1) the Northern Mid-latitudes [35-55°N] and (2) the Southern Mid-latitudes [35°S-65°S]. Trial wave model simulations were then carried out in which various factoring schemes were applied to the higher wind speeds (>10 m/s). The model results were then interpolated to each and every Topex data point in the regional boxes. The goodness of fit was evaluated by means of quantile-quantile wave height

comparisons over the range from 1% to 99.95%. Figure 5 shows q-q plots for the southern mid-latitudes before and after the wind speed factoring was applied.
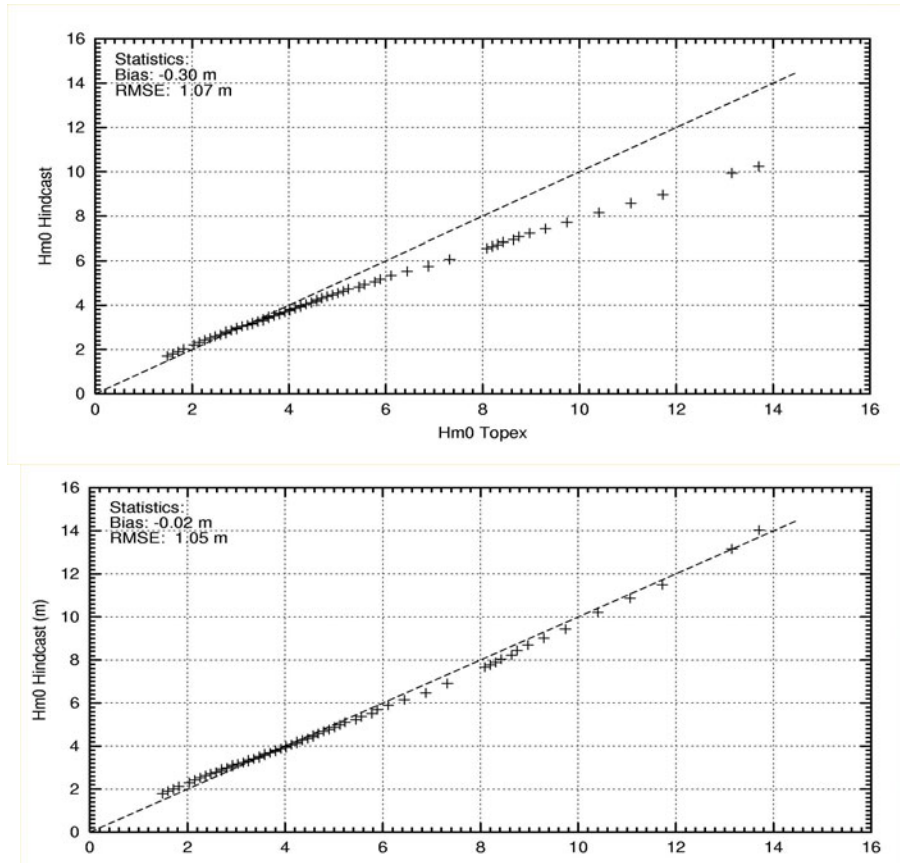

Figure 5. Effect of Wind Speed Factoring on Quantile-Quantile Lower Mid-Latitudes.
Top plot is unfactored winds while the bottom plot includes factored winds.

The wind speed factoring ultimately applied to the model had the following form:

Northern Region: $\qquad$ $U_{model} = U_{NCEP} * (1 + (U_{NCEP}-14.5)*0.026)$
Southern Region: $\qquad$ $U_{model} = U_{NCEP} * (1 + (U_{NCEP}-13.5)*0.027)$

Where U_{model} is the wind speed input to the wave model and U_{NCEP} is the 10 m interpolated NCEP wind speed.

5.2 Swell Propagation and Computational Requirements

The appropriate simulation of the propagation of ocean swell waves has proven problematic in wave models due to practical limitations in model resolution in both physical and spectral space. In the latter case, as the energy spectrum in a numerical wave model is divided into a discrete number of frequency and directional bands, continuous fields of swell waves fragment into discrete parcels of energy as they propagate in space. This fragmentation is known as the Garden Sprinkler Effect (GSE).

A series of numerical experiments were conducted to assess various methodologies for alleviating the GSE. This phenomenon has been explored by others (for example, Booij and Holthuijsen (1987); Tolman (2001)); however, in our case there was a strong emphasis on computational speed. The original WAVAD model, which utilizes a standard first order upwind propagation scheme, is a highly efficient model. For the Pacific Ocean (160x132 grid), a ten-year simulation required only 50 hours of computational time on a Pentium4 1.4 GHz personal computer. However, the first order scheme was found to be excessively diffusive and did not appropriately rid the model of

GSE. In our investigations, there was a strong emphasis on addressing the GSE without significantly compromising the existing computational speed of the model. The concern is that if computational requirements became too lengthy, this would limit the degree of investigation and model testing that could be applied in other areas of the study, such as wind field development. Thus, the accuracy requirements of any given scheme were carefully weighed against the computational penalty.

Booij and Holthuijsen (1987) recognized the need for a diffusion operator to counteract the limitations of a discrete frequency and direction spectrum, and introduced a diffusion correction into the basic equations defining wave propagation. This approach did have the requirement of defining an appropriate "wave age", or time lapsed since generation of the waves, for the wave fields under consideration, and can have the undesirable effect of potentially influencing the model time step, depending on the model resolution. Tolman (2001) explored other approaches to correcting for GSE, including the use of both a simple box averaging scheme and an approach in which divergence was added to the advection velocities.

Both of these previous studies made the point of starting with a highly accurate propagation scheme to which the diffusion operator was then applied that "smears" this highly accurate solution in space to address GSE issues. This has the important effect of giving a controllable diffusion. Given our concerns with model computational speed, we sought an approach that improved the numerics of WAVAD beyond first order but did not come the computational demands of a high order scheme. That is, a certain degree of numerical diffusion was acceptable in the propagation scheme given that a diffusion operator would subsequently be applied to address GSE.

Some of the numerical schemes investigated in our study included:

- First order downwind interpolation.
- Modified second order Lax-Wendroff.
- Third order QUICKEST/ULTIMATE.

The ULTIMATE scheme, which has been employed by Tolman (2001) in WAVEWATCH III, was the most accurate of the schemes considered and was used as the starting point in the study and as a base case for the comparisons. This scheme, although efficient, placed significant computational demands that other alternatives were explored.

The Garden Sprinkler Effect was addressed using Tolman's averaging scheme due to its efficiency. In this approach, the energy at each grid point was estimated by averaging the wave energy at the four corners of a box of dimensions $\alpha \Delta C_g \Delta t$ and $\beta Cg \Delta \theta \Delta t$ surrounding the grid point, with the corner values estimated by means of bi-linear interpolation. Cg is defined as the wave group speed; $\Delta \theta$, the directional resolution and Δt, the time step. Two tunable parameters, α and β, were ultimately set to 2.0 and 4.0, respectively.

One of the primary numerical tests was based on the work of Booij and Holthuijsen (1987) and subsequent investigations of Tolman (2001). A wave model grid of dimensions of 100 degrees by 100 degrees (11,100 x 11,100 km) was established with a 1-degree resolution. An initial maximum wave height of 7.0 m was applied in the model in the lower left region of the grid (Point 12,12). The waves had a mean direction of 30° with $\cos^2$ directional distribution and a peak period of 10 seconds. The wave height distribution was Gaussian in space with an overall radius of 200 km. A time step of 1 hour was employed.

Figure 6 provides a summary of results for a few selected cases. Figure 6a shows a solution for the test case after a 7 day time period if a one-degree directional resolution is utilized in the wave model. Figure 6b illustrates the fragmentation of the GSE when a reduced directional resolution, 15 degrees, is utilized.

The results of a simulation using the Lax-Wendroff scheme in conjunction with the Tolman smoothing approach is shown in Figure 6c. Some of the GSE is still discernable but the solution is much improved as compared to the solution without smoothing.

It was observed, based on these and other numerical experiments, that the GSE could be reduced to some degree by means of a higher order numerical propagation scheme in conjunction with the Tolman smoothing. In terms of

computational time, the existing first order scheme (without smoothing) was found to be the most efficient by a significant margin. The Lax-Wendroff scheme, in combination with the smoothing, took approximately 3.5 times longer than the first order approach. The QUICKEST/ULTIMATE scheme required twice the computer time of the Lax-Wendroff scheme.

The first order downwind scheme was highly efficient but did not perform as well as other approaches due to the excessive numerical diffusion of this scheme. Interestingly, the relative merits of this scheme were improved when great circle effects were considered in the computations. Figure 6d shows an example solution for the first order scheme when curvature is included.

The general conclusions from our experimentation were:

- A second order scheme in combination with a diffusion operator is likely sufficient for improving the overall accuracy of swell propagation without placing an excessive computational burden on a 2nd generation wave model.
- Concepts and approaches to the development of an efficient GSE diffusion operator need to be improved.

Ultimately, the first order downwind scheme was selected for initial application to the Pacific Ocean and the results presented in this paper are based on these results; however, efforts are continuing to improve the propagation numerics in WAVAD.

(a) QUICKEST/ULTIMATE – 1 degree directional resolution

(b) QUICKEST/ULTIMATE – 15 degree directional resolution

(c) Lax-Wendroff with Tolman Bin Smoothing
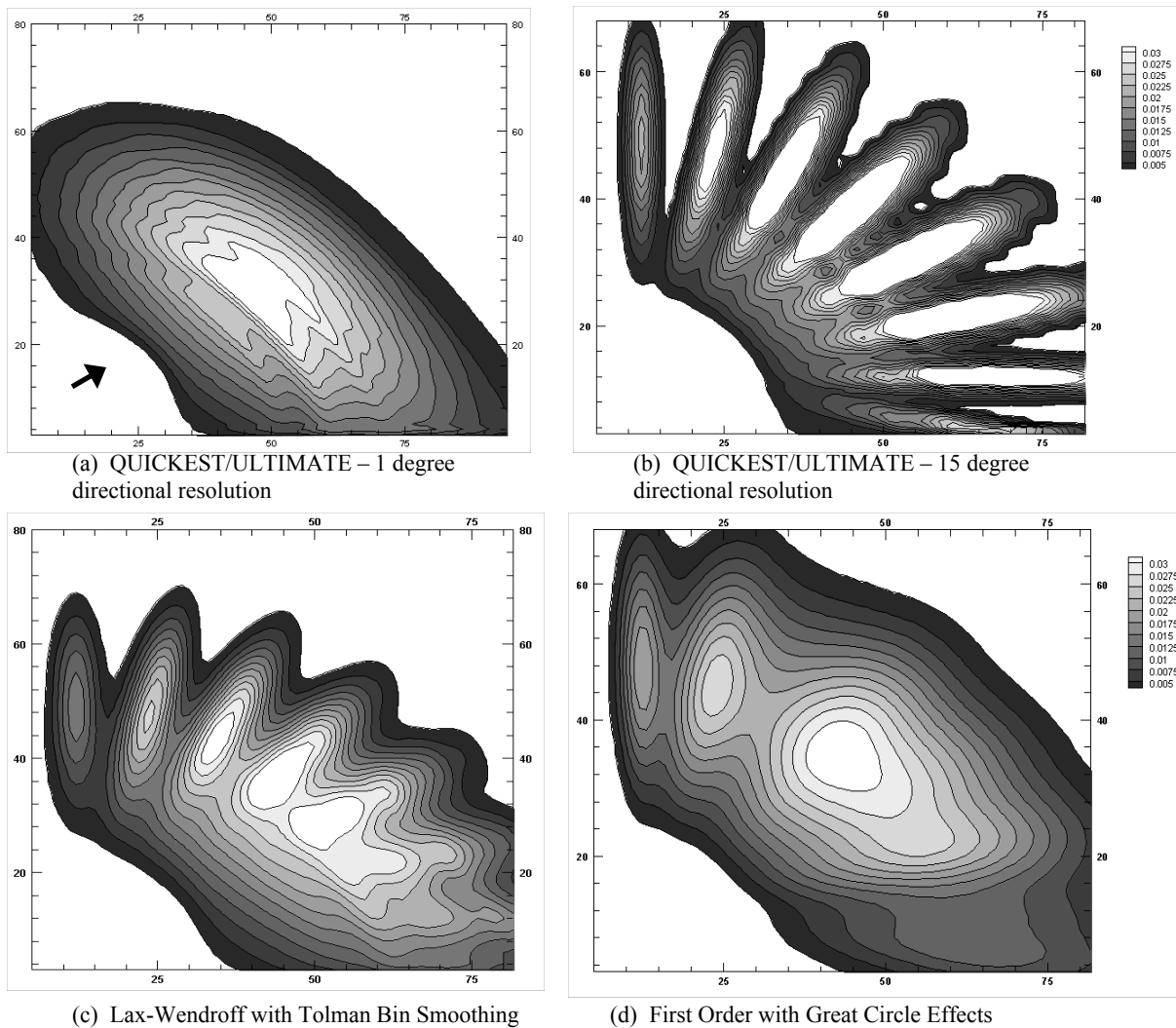
(d) First Order with Great Circle Effects

Figure 6. Contours of Energy from Experimentation with Wave Model Propagation Schemes
[After 7 days of simulation; Grid dimensions in degrees; Contour interval=25 cm^2]

6. MODEL VALIDATION

A forty-year hindcast for the time period from 1961 to 2000 was performed, and the results validated against all available measurements. Table 2 summarizes the comparisons with the Topex measurement locations while Table 3 gives comparisons to the historical recorded buoy data.

It is important to note that detailed examination of the recorded buoy data showed that many of these buoys were located adjacent to quite complex shoreline configurations. To properly transform the deep water waves to each site would have required comprehensive shallow water modelling; however, this level of effort was beyond the scope of the study. For this investigation, the spectral wave data were transformed to the buoy locations using simplistic means (Snell's Law), thus, the comparisons are only of limited accuracy.

The hindcast showed some distinct spatial trends with an underestimation of the wave climate in the south to a overestimate in the north. A short period of directional spectral data were available for the Valparaiso region. A comparison of these data confirmed our suspicions that the model was potentially creating excessive swell in the North Pacific.

Based on the validation results, some short term (1 year) simulations have been carried out implementations of the various numerical schemes outlined in Section 5. These subsequent comparisons have shown that the swell over-estimate may be primarily attributable to the inadequacies of the propagation scheme. It was also identified that the overall spectral spreading was too large, and various steps will be taken to correct this in the model. As a result, the hindcast will be re-run in the near future.

Table 2
Wave Model Comparisons to Topex Satellite Data

Topex Location	Bias (m)	RMSE (m)	Scatter Index
1	0.04	1.14	27%
2	-0.05	0.97	23%
3	-0.10	0.85	23%
4	-0.12	0.78	24%
5	-0.15	0.74	25%
6	-0.15	0.74	26%
7	-0.04	0.70	26%
8	-0.09	0.70	28%
9	0.11	0.62	28%
10	0.25	0.60	26%
11	0.29	0.54	23%
12	0.03	0.62	23%

Table 3
Wave Model Comparisons to Wave Buoy Data

Buoy Location	Hm0 (m)		Tp (s)	
	Bias	RMSE	Bias	RMSE
Arica	0.32	0.55	0.8	3.1
Iquique	0.29	0.54	1.0	4.1
Caldera	0.57	0.72	0.9	3.9
Coquimbo	0.09	0.53	1.4	3.8
Valparaiso (1979-81)	-0.14	0.64	0.6	4.0
Valparaiso (2000)	0.32	0.72	3.0	4.4
Constitucion	0.28	0.65	1.4	4.7
Golfo Coronados	0.46	0.91	2.4	5.2

Note: Wave buoys generally located in shallow water with exposure limitations. Detailed shallow water wave modelling was not performed.

7.   PRESENCE OF MULTI-DIRECTIONAL WAVE CONDITONS AND NEARSHORE WAVE
TRANSFORMATION

As noted previously, one of the interests in this work was on the relative contributions of northern and southern
swells to the wave climate along the Chilean coast. Comprehensive directional wave measurements for Chile are
not yet available, thus, the wave model provides an initial indication of the importance of swell to coastal
infrastructure design.

As a first step towards developing an understanding of swell impacts, a procedure for isolating the individual wave
systems from the wave model directional spectra was developed based on the work of Hanson and Phillips (2001).
Basically, the procedure breaks down each individual spectrum into subsets representing each of the sea and swell
wave components. The following steps were carried out in the process:

1. Each peak in the computed spectra is isolated by means of spectral partitioning using a steepest ascent
    algorithm ("queen's move" ascent).
2. The peaks associated with wind seas are identified and combined based on a wave age criterion.
3. Adjacent swell peaks were evaluated to see if they derived from the same wave system based on criteria
    established regarding directional spreading, peak separation and minimum energy between peaks.

In this study, low-energy wave components were not considered; only those spectral partitions with an equivalent of
characteristic wave height of greater than 0.5 m were included. An analysis was then performed to determine the
frequency that waves arrive from two or more directions with an angular separation of 45 degrees or greater.

Figure 7 shows the percentage of time that multi-directional waves occur for locations along the Chilean coastline
going from north (left on x-axis) to south (right).   The very high percentage of time that more than one wave system
influences the wave climate in Chile may be seen. There is also an increasing trend in multi-directionality from
north to south. Part of the sharp change in multi-directionality in the north end of the country may be associated
with the northern sheltering created by the western "bulge" of South America.

A more detailed examination of the various spectral peaks isolated in the data set showed that not all of the multi-
directionality was associated with north and south swell systems, particularly in the southern part of the coastline.
In the south, the local seas typically are generated by western winds, but swell waves can arrive from a more
southerly direction.

It is also interesting to examine the seasonal variation of the multi-directional wave conditions, as shown in Figure 8
for three selected locations. It may be noted that wave conditions are less complex in the Southern Hemisphere
winter months when Northern Pacific wave conditions are less severe. The seasonal effect is smaller in the south
than in the north.

Clearly, part of the multi-directionality may be attributed to issues of simulation of northern swell and a possible
over-estimation of the magnitude of these swells. Nevertheless, the complexity of the wave climate in Chile is
apparent, and this has many implications with respect to how nearshore wave transformation should be performed.
It is important that the multi-modal nature of the waves be considered in shallow water modeling procedures, and
that summary parameters, such as the Mean Wave Direction, are not meaningful in this context.
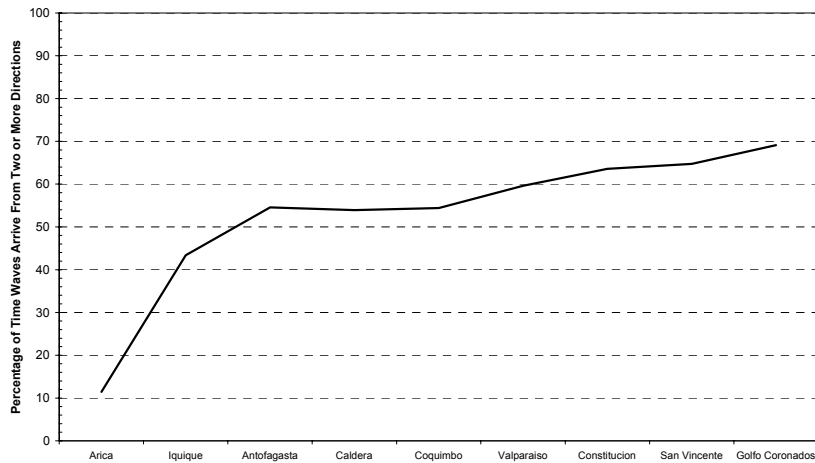
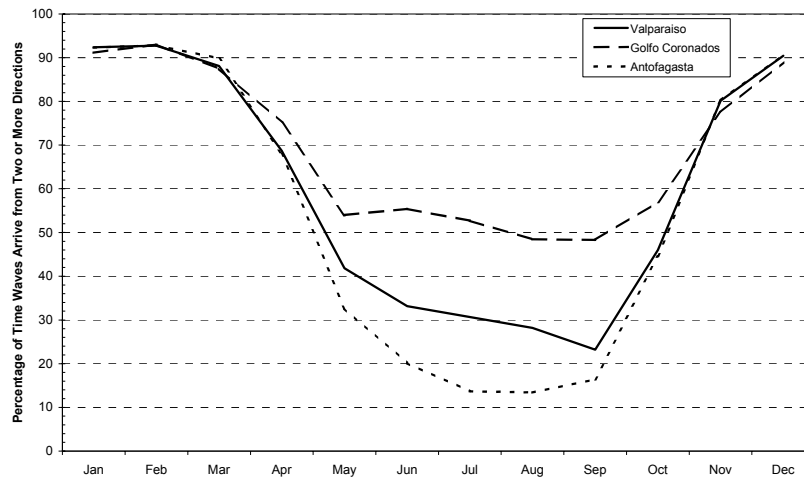Figure 7. Frequency that Waves Arrive from More than One Direction

Figure 8. Annual Variation in Frequency of Multi-Directional Wave Conditions

8.   CONCLUSIONS

An investigation into swell wave conditions in the southern Pacific Ocean has been carried out by means of 40-year wave hindcast using a 2nd generation wave model and wind fields derived from the NCEP/NCAR Re-analysis Project. The wave studies have clearly shown the complexity and multi-directional nature of the wave conditions offshore of Chile, which has important implications with respect to nearshore climate, and may significantly impact coastal engineering works, including port design and sediment transport analyses.

Some initial studies of wave propagation schemes and their impact on the wave modeling results have been completed with particular emphasis on model computational speed. Various concepts and approaches to the development of an efficient diffusion operator to address Garden Sprinkler Effect need to be addressed.

Further efforts to improve both the wave model and the Pacific Ocean hindcast are continuing.

This study has provided a direction for future wave measurement initiatives in Chile. Another outcome of this work has been the development of a draft "norm", or standard, for wave analysis work in Chile. This norm will outline the minimum level of technical investigation, and provides specific mention of the requirement for appropriate analysis of the complex wave conditions present along the Chilean coastline.

9.   ACKNOWLEDGEMENTS

10. REFERENCES

Booij, N. and Holthuijsen, L.H. 1987. Propagation of Ocean Waves in Discrete Spectral Wave Models. J. Computer Physics. Vol. 68. pp. 307-326.

Cotton, P.D. 2001. Topex B Side Altimeter Wind Speed and Significant Wave height Calibration (1999-2000). December.

Cox et al., 1998 : Evaluation of NCEP/NCAR Reanalysis Project Marine Surface Wind Products for a Long Term North Atlantic Wave Hindcast. Proceedings of the 5th International Workshop on Wave Hindcasting and Forecasting. Melbourne, Fl. January 26-30.

Hanson, J.L. and Phillips, O.M. 2001. Automated Analysis of Ocean Surface Directional Wave Spectra. Journal of Atmospheric and Oceanic Technology. February. pp. 277-293.

Kalnay, E. et al. 1996 : The NCEP/NCAR 40-Year Reanalysis Project. Bull. AMS. 77(3). 437-471.

Hanson, J.L. and Phillips, O.M. 2001. Automated Analysis of Ocean Surface Directional Wave Spectra. Journal of Atmospheric and Oceanic Technology. February. pp. 277-293.

Leonard, B.P. (1979). A Stable and Accurate Convective Modelling Procedure Based on Quadratic Upstream Interpolation. Computer Methods Appl. Mech. Eng. 19.

Leonard, B.P. (1991). The ULTIMATE Conservative Difference Scheme Applied To Unsteady One-dimensional Advection. Computer Methods Appl. Mech. Eng. 88.

Resio, D. and Perrie, W. (1989). Implications of an f^4 Equilibrium Range for Wind-Generated Waves, Journal of Physical Oceanography. Volume 19. pp. 193-204. February.

Resio, D. (1981). The Estimation of Wind-Wave Generation in a Discrete Spectral Model. Journal of Physical Oceanography. Vol. 11, No. 4.

Tolman, H.L. 2001. Improving Propagation in Ocean Wave Models. Ocean Wave Measurement and Analysis. San Francisco.   pp. 507-516.